Bond dissociation energies of diatomic transition metal selenides: TiSe, ZrSe, HfSe, VSe, NbSe, and TaSe

Jason J. Sorensen, Thomas D. Persinger, Andrew Sevy, Jordan A. Franchina, Eric L. Johnson, and Michael D. Morse[a)]
Department of Chemistry, University of Utah, Salt Lake City, Utah 84112, USA

(Received 7 September 2016; accepted 12 November 2016; published online 2 December 2016)

Predissociation thresholds have been observed in the resonant two-photon ionization spectra of TiSe, ZrSe, HfSe, VSe, NbSe, and TaSe. It is argued that the sharp onset of predissociation corresponds to the bond dissociation energy in each of these molecules due to their high density of states as the ground separated atom limit is approached. The bond dissociation energies obtained are D_0(TiSe) = 3.998(6) eV, D_0(ZrSe) = 4.902(3) eV, D_0(HfSe) = 5.154(4) eV, D_0(VSe) = 3.884(3) eV, D_0(NbSe) = 4.834(3) eV, and D_0(TaSe) = 4.705(3) eV. Using these dissociation energies, the enthalpies of formation were found to be $\Delta_{f,0K}H^o$(TiSe(g)) = 320.6 ± 16.8 kJ mol^{-1}, $\Delta_{f,0K}H^o$(ZrSe(g)) = 371.1 ± 8.5 kJ mol^{-1}, $\Delta_{f,0K}H^o$(HfSe(g)) = 356.1 ± 6.5 kJ mol^{-1}, $\Delta_{f,0K}H^o$(VSe(g)) = 372.9 ± 8.1 kJ mol^{-1}, $\Delta_{f,0K}H^o$(NbSe(g)) = 498.9 ± 8.1 kJ mol^{-1}, and $\Delta_{f,0K}H^o$(TaSe(g)) = 562.9 ± 1.5 kJ mol^{-1}. Comparisons are made to previous work, when available. Also reported are calculated ground state electronic configurations and terms, dipole moments, vibrational frequencies, bond lengths, and bond dissociation energies for each molecule. A strong correlation of the measured bond dissociation energy with the radial expectation value, $\langle r \rangle_{nd}$, for the metal atom is found. *Published by AIP Publishing.* [http://dx.doi.org/10.1063/1.4968601]

I. INTRODUCTION

The making and breaking of chemical bonds are arguably the most fundamental processes in all of chemistry. The transition metals are of particular interest in this regard, as they are often employed to facilitate the controlled formation of new chemical bonds, especially in the fields of organometallic chemistry, surface chemistry, and catalysis. Thus, the nature of transition metal bonding to main group atoms is an area of great interest. The chemical bonding between transition metals and selenium is of technological interest in several fields, including pseudocapacitor electrodes,[1] semiconductors,[2] and electrocatalysts.[3,4] Despite this interest in bulk transition metal selenides, little is known about the more fundamental chemical bonding in diatomic transition metal selenides. To our knowledge, only two diatomic transition metal selenides have received any spectroscopic scrutiny at all, with spectroscopic studies published only on MnSe[5] and CuSe.[6]

One of the grand goals of computational chemistry is to predict accurately the thermochemistry and activation energies of chemical reactions, so that improvements in our understanding of reaction mechanisms and kinetics, and ultimately in catalyst design, may be made. To model such reactions satisfactorily, the computational method must be able to represent each step along the reaction path accurately, including reactants, products, and all applicable transition states. Accurate calculations of the energetics of the reactants and products permit the thermochemistry to be derived, while accurate calculations of the transition state are necessary to model reaction kinetics. As the transition state often corresponds to a partially dissociated system, computational methods that fail to calculate bond dissociation energies (BDEs) accurately may also fail to provide accurate values for transition state energies. Thus, the computation of accurate thermochemistry is a key goal of computational chemistry.

Even though BDEs are among the most useful quantities that computational chemistry can provide, highly accurate computational methods, particularly methods that can be scaled to treat larger systems, remain elusive. This is because of the difficulty in treating electron correlation in the initial molecule to the same level of accuracy as in the dissociated products. This is often possible for systems composed of main group elements; the increased electronic complexity in the *d*- and *f*-block metals presents significant difficulties for current computational methods, however.[7–9]

One of the significant obstacles in improving current theoretical methods is the lack of precisely determined experimental BDEs to serve as points of comparison. Such precise values set a standard upon which various computational methods may be tested for accuracy.[7–9] Computational methods are considered to have achieved "chemical accuracy" if the thermochemical property can be computed to within 1.0 kcal mol^{-1} (0.04 eV) of experiment.[10] This result may be achieved for many main group molecules. On the other hand, for the more difficult transition-metal containing molecules, the accepted tolerance for "chemical accuracy" is within 3.0 kcal mol^{-1} (0.13 eV) of experiment due to the greater difficulties associated with these species.[10] A significant challenge is that many experimental values themselves are not known to this level of certainty, and in some cases error limits may be significantly underestimated. To alleviate this deficit, in a recent publication, we have reported the BDEs of VC, VN, and VS to a

a)Author to whom correspondence should be addressed. Electronic mail: morse@chem.utah.edu

precision of 0.003 eV, or better.[11] In this article, we extend this work to provide BDEs of TiSe, ZrSe, HfSe, VSe, NbSe, and TaSe, measured by the observation of a sharp predissociation threshold in the resonant two-photon ionization (R2PI) spectra of these molecules. As in our previous measurements,[11] all reported values have an accuracy that is well within the required "chemical accuracy" of main group compounds.

Very little previous work has been reported on these diatomic transition metal selenides. Of the molecules investigated here, the BDE has been previously measured only for VSe.[12] An estimated BDE for TiSe has also been reported,[13] based on extrapolation from experimental values of other titanium-containing compounds. In addition, Wu, Wang, and Su have computed BDE values for TiSe and VSe using density functional theory (DFT) calculations.[14] The ground states of TiSe and VSe were also calculated by Wu, Wang, and Su to be $^3\Delta$, corresponding to the $1\sigma^2\ 2\sigma^2\ 1\pi^4\ 1\delta^1\ 3\sigma^1$ configuration, and $^4\Sigma^-$, corresponding to the $1\sigma^2\ 2\sigma^2\ 1\pi^4\ 1\delta^2\ 3\sigma^1$ configuration, respectively.[14] Here, the orbital numbering scheme only includes valence molecular orbitals that derive primarily from the atomic valence orbitals (3*d* and 4*s* on Ti or V, 4*s* and 4*p* on Se).

To date, there have been no spectroscopic studies on any of these molecules, so there are no experimental data available that could be used to deduce the ground terms. When rotationally resolved spectra are available, it is possible to deduce that ground state Ω'' value experimentally, which places severe constraints on the possible term symbol, and as a result, on the ground molecular configuration of the molecule. In many cases, the observed Ω'' value constrains the choices sufficiently that only a single configuration and term are plausible. Unfortunately, the lack of rotationally resolved spectra prevents such a determination for the molecules considered here. As no previous work of any kind has been reported on ZrSe, HfSe, NbSe, or TaSe, density functional calculations have been performed on all six molecules, and the results are presented.

II. EXPERIMENTAL

Hydrogen selenide gas was synthesized by acid hydrolysis of ZnSe powder in an apparatus that was slowly flushed with helium. Concentrated HCl was added to a flask containing ZnSe powder and was gently heated. The resulting H_2Se vapor was carried by the He flow through a $CaCl_2$ drying tube to remove water vapor and then was passed through two liquid nitrogen traps (−196 °C), which condensed the H_2Se product. When the reaction had stopped, the traps were evacuated while the product remained frozen. At that point, the traps were connected to an evacuated gas cylinder and were allowed to warm to room temperature, filling the gas tank with hydrogen selenide gas. The H_2Se was then diluted with helium to approximately 0.25% H_2Se by pressure.

The experimental process is identical to our previous work on VC, VN, and VS.[11] A metal disk of Ti, Zr, Hf, V:Mo (1:1), Nb, or Ta was laser ablated by the third harmonic output of a Nd:YAG laser (355 nm). The metal samples were rotated and translated to ensure that holes were not drilled into the sample and that the molecule production remained reasonably stable. The resulting metal plasma was then carried by a pulse of the H_2Se gas mixture through a 1.3 cm long reaction zone before undergoing supersonic expansion into vacuum from a 3 mm orifice, cooling the gaseous reaction products to about 10 K.

The expanding gas was skimmed to 1 cm in diameter as it passed into the second chamber. The beam was then exposed to tunable laser radiation in the range of 300-234 nm produced by an optical parametric oscillator (OPO) laser, which was counterpropagated along the molecular beam. After approximately 20 ns, radiation from a KrF excimer laser (248 nm, 5.00 eV), directed perpendicular to the molecular beam, was used to ionize the species in the beam. The resulting ions were then accelerated in a Wiley-McLaren ion source into a reflectron time-of-flight mass spectrometer.[15,16] Ion signals were measured with a microchannel plate detector, preamplified, and digitized for further processing. The process was repeated at a rate of 10 Hz, and 30 shots were averaged for each wavelength point. To improve the signal to noise ratio, three to four scans were averaged for each spectrum.

III. COMPUTATIONS

All calculations were performed in Gaussian 09[17] using the B3LYP density functional theory method[18,19] and the LANL2DZ basis set.[20] This basis set utilizes an effective core potential (ECP), which was parameterized to reproduce calculations that treated the core terms with the inclusion of scalar relativistic effects, in particular the mass-velocity and Darwin relativistic terms. The ECP treats each of these atoms somewhat differently. For Ti and V, it treats electrons through [Ne] as core electrons. For Se, Zr, and Nb, the core electrons are [Ar] plus the 3d electrons. Lastly, Hf and Ta have [Kr] plus 4d and 4f electrons treated in the core potential.

Unrestricted optimization and frequency calculations were performed to deduce the ground state configurations for each metal selenide along with bond lengths, dipole moments, vibrational frequencies, and BDEs. All calculations were performed in the C_{2v} point group and neglected spin orbit coupling. In each case, two proposed ground state configurations were tested to see which lay lower in energy. For TiSe, ZrSe, and HfSe, the proposed ground states were $1\sigma^2\ 2\sigma^2\ 1\pi^4\ 1\delta^1\ 3\sigma^1$, $^3\Delta$ and $1\sigma^2\ 2\sigma^2\ 1\pi^4\ 3\sigma^2$, $^1\Sigma^+$ based on trends observed in their corresponding oxide[21–23] and sulfide[24–26] ground states. For VSe, NbSe, and TaSe, similar trends in their respective oxides[27–29] and sulfides[30–32] were used to deduce that the probable ground states were $1\sigma^2\ 2\sigma^2\ 1\pi^4\ 1\delta^2\ 3\sigma^1$, $^4\Sigma^-$ and $1\sigma^2\ 2\sigma^2\ 1\pi^4\ 3\sigma^2\ 1\delta^1$, $^2\Delta$.

IV. RESULTS

A. Computations

Table I displays the dipole moments (μ, Debye), vibrational frequencies (ω_e, cm^{-1}), bond lengths (r_e, Å), term energies (T_e, eV), and DFT predicted BDEs (D_0, eV) obtained for TiSe, ZrSe, HfSe, VSe, NbSe, and TaSe. These values were calculated for each molecule considering only the two proposed spin multiplicities indicated above. Term energies are reported relative to the calculated ground term. Table I also provides a spin-orbit corrected value of the BDE in the last

TABLE I. Calculated molecular configurations and terms and molecular properties for TiSe, ZrSe, HfSe, VSe, NbSe, and TaSe. These results are reported for the two most likely candidates for the ground state.

Molecule	Electronic term	Term energy, T_e (eV)[a]	Dipole moment, μ (Debye)	Vibrational frequency, ω_e (cm^{-1})	Bond length, r_e (Å)	Dissociation energy, D_0 (eV)	Spin-orbit corrected D_0 (eV)[b]
TiSe	$1\delta^1 3\sigma^1, {}^3\Delta\ (\Omega = 1)$	0	6.11	399	2.255	4.082	3.952
	$3\sigma^2, {}^1\Sigma^+\ (\Omega = 0^+)$	1.27	4.40	445	2.186	2.810	2.665
ZrSe	$1\delta^1 3\sigma^1, {}^3\Delta\ (\Omega = 1)$	0	5.69	359	2.372	4.699	4.540
	$3\sigma^2, {}^1\Sigma^+\ (\Omega = 0^+)$	0.43	4.07	383	2.330	4.264	4.057
HfSe	$3\sigma^2, {}^1\Sigma^+\ (\Omega = 0^+)$	0	4.20	340	2.319	4.763	4.306
	$1\delta^1 3\sigma^1, {}^3\Delta\ (\Omega = 1)$	0.53	5.71	316	2.356	4.237	3.976
VSe	$1\delta^2 3\sigma^1, {}^4\Sigma^-\ (\Omega = 1/2, 3/2)$	0	5.84	368	2.246	3.710	3.553
	$1\delta^1 3\sigma^2, {}^2\Delta\ (\Omega = 3/2)$	1.27	4.07	386	2.184	2.443	2.308
NbSe	$1\delta^2 3\sigma^1, {}^4\Sigma^-\ (\Omega = 1/2, 3/2)$	0	4.83	360	2.316	4.167	3.971
	$1\delta^1 3\sigma^2, {}^2\Delta\ (\Omega = 3/2)$	0.70	4.67	374	2.304	3.469	3.338
TaSe	$1\delta^1 3\sigma^2, {}^2\Delta\ (\Omega = 3/2)$	0	3.15	350	2.274	4.101	3.788
	$1\delta^2 3\sigma^1, {}^4\Sigma^-\ (\Omega = 1/2, 3/2)$	0.11	4.69	330	2.306	3.997	3.437

[a]Term energies ignore spin-orbit interaction, which stabilizes the lowest Ω-level, particularly for Δ terms involving the 5*d* metals HfSe and TaSe.
[b]See Section V D 2 for a description of how the spin-orbit correction to D_0 was estimated.

column. See Section V D 2 for an explanation of how this correction was estimated.

In these molecules, we number the molecular orbitals based on the valence n*d* and (n + 1)*s* orbitals of the metal atom and the valence 4*s* and 4*p* orbitals of selenium. A qualitative molecular orbital diagram is presented in Figure 1. The 1σ orbital is primarily core-like and is dominated by a selenium 4*s* character. The 2σ and 1π orbitals are the bonding orbitals that are primarily linear combinations of the metal *nd*σ and *nd*π orbitals with the corresponding 4*p*σ and 4*p*π orbitals of selenium. All of these are filled in the low-lying states of the investigated molecules. Lying above these are the 1δ and 3σ orbitals, which are composed primarily of metal *nd*δ and (n + 1)*s* character, respectively, and are best characterized as nonbonding. Finally, at higher energies are the 2π and 4σ orbitals, which are the antibonding combinations of the *nd*π and *nd*σ orbitals, respectively, with the selenium 4*p*π and 4*p*σ orbitals. The candidates for the ground states in the investigated molecules fill the 1σ, 2σ, and 1π orbitals and place the remaining two or three electrons in the nonbonding 1δ or 3σ orbitals. In our discussions of the isovalent oxides and sulfides, we use the same numbering scheme for the molecular orbitals that derive from the valence orbitals of oxygen (2*s*, 2*p*) or sulfur (3*s*, 3*p*). As one might expect, the relative energies of these orbitals, particularly the 3σ and 1δ orbitals, vary as one moves from one metal to another.

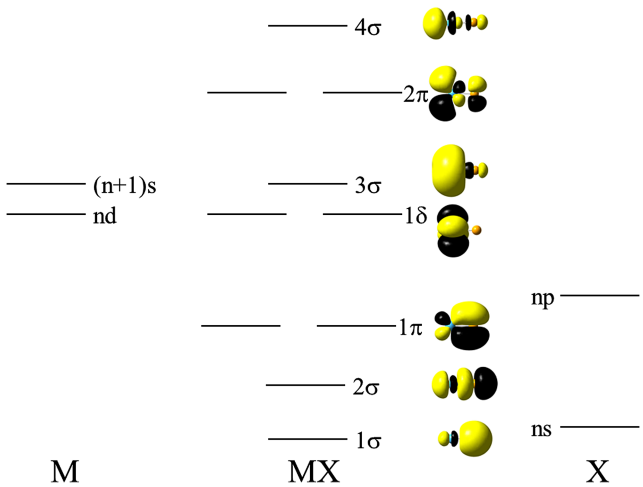

FIG. 1. Qualitative molecular orbital diagram for the transition metal selenides. The molecular orbitals displayed were calculated for HfSe. Orbital energies are not to scale.

The experimentally determined ground states of TiO and TiS are $1\sigma^2\ 2\sigma^2\ 1\pi^4\ 1\delta^1\ 3\sigma^1, {}^3\Delta_1$,[21,24] which also emerges as the computationally predicted ground state of TiSe. Similarly, the experimentally determined ground states of VO and VS are both $1\sigma^2\ 2\sigma^2\ 1\pi^4\ 1\delta^2\ 3\sigma^1, {}^4\Sigma^-$,[27,30] as is computationally found for VSe. In fact, throughout the entire set of six metals, experiment finds that the corresponding MO and MS molecules always have the same ground electronic configuration and term, and in every case except for Zr, our computed ground configuration and term for the MSe species agrees with the known ground term of the MO and MS molecules. In the lighter members of a given group, the metal *s*-like 3σ orbital is singly occupied, leading to ground terms of $1\sigma^2\ 2\sigma^2\ 1\pi^4\ 1\delta^1\ 3\sigma^1, {}^3\Delta_1$, in TiO,[21] TiS,[22] and in our calculations of TiSe and ZrSe. Similarly, in the lighter group 5 chalcogenides VO,[27] VS,[30] NbO,[28] NbS,[31] and calculated in VSe and NbSe, the ground term is $1\sigma^2\ 2\sigma^2\ 1\pi^4\ 1\delta^2\ 3\sigma^1, {}^4\Sigma^-$, again leaving the 3σ orbital singly occupied. In the 5d metal chalcogenides, relativistic stabilization of the 6s orbital leads to double occupation of the 3σ orbital, giving ground terms of $1\sigma^2\ 2\sigma^2\ 1\pi^4\ 3\sigma^2, {}^1\Sigma^+$ in HfO,[23] HfS,[26] and calculated in HfSe, and ground terms of $1\sigma^2\ 2\sigma^2\ 1\pi^4\ 3\sigma^2\ 1\delta^1, {}^2\Delta_{3/2}$ in TaO,[29] TaS,[32] and calculated in TaSe.

The unusual situation occurs in ZrSe, where our calculation identifies the ground state to be $1\sigma^2\ 2\sigma^2\ 1\pi^4\ 1\delta^1\ 3\sigma^1, {}^3\Delta_1$, as opposed to the experimentally known $1\sigma^2\ 2\sigma^2\ 1\pi^4\ 3\sigma^2, {}^1\Sigma^+$ ground states of ZrO and ZrS.[22,25] We do not consider our results to be definitive for ZrSe, in part because we were only concerned with identifying the singlet and triplet candidates for the ground state, not establishing their definitive energy ordering. To computationally determine the energy ordering would require a more sophisticated calculation, which was

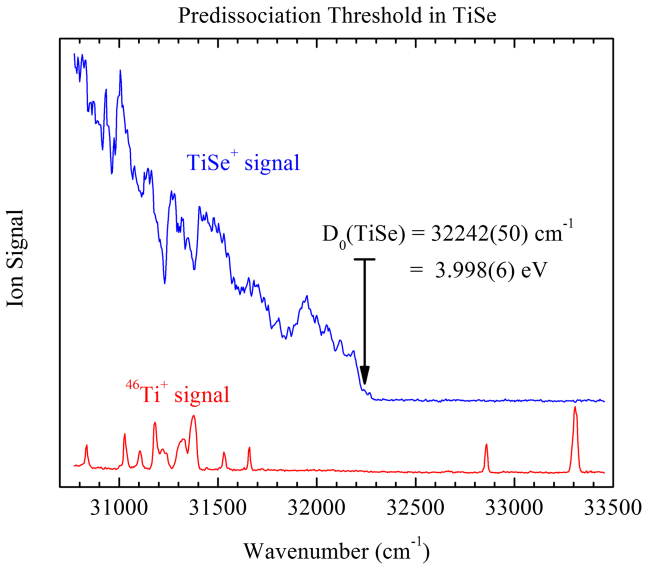

FIG. 2. Resonant two-photon ionization spectrum of $^{48}Ti^{80}Se$ (blue) along with the spectrum of the minor isotope ^{46}Ti (red), which was used for calibration.

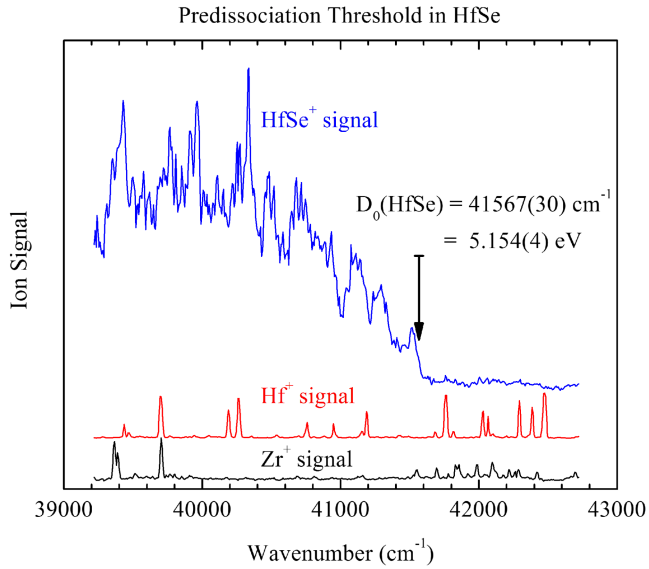

FIG. 4. Resonant two-photon ionization spectrum of $^{178}Hf^{80}Se$ (blue) along with the spectrum of the impurity ^{90}Zr (black) and the minor isotope ^{174}Hf, which were used for calibration.

beyond the scope of this investigation. In addition, the known $^3\Delta_1$-$^1\Sigma^+$ separation in ZrO (1080 cm^{-1})[33] is much smaller than in TiO (2973 cm^{-1}),[34] HfO (9231 cm^{-1}),[23] or HfS (6631 cm^{-1}).[26] This suggests that the corresponding splitting in ZrS and ZrSe will also be small, making a definitive computational assignment of the ZrSe ground state more problematic than for the other molecules.

B. Bond dissociation energies and enthalpies of formation

Displayed in Figures 2–7 are the R2PI spectra of TiSe, ZrSe, HfSe, VSe, NbSe, and TaSe near the predissociation threshold along with the atomic transitions that were used for calibration. With the possible exception of TiSe, in all cases the predissociation threshold is clearly identified by an abrupt drop to baseline, with negligible ion signal above the threshold. In the case of TiSe, a weak shoulder persists a bit above the sharp drop; we have increased our proposed error limit to include this shoulder. In all cases, the proposed error limit is indicated by the horizontal bar that lies at the top of the arrow indicating the location of the threshold.

The bond dissociation energies, D_0, are tabulated in Table II for each metal selenide. The standard enthalpies of formation for each gaseous metal selenide, $\Delta_{f,0K}H^o(MSe(g))$ are also listed. These were determined using the BDEs determined in this work along with the standard enthalpies of formation for each gaseous metal, $\Delta_{f,0K}H^o(M(g))$, as found in the fourth edition JANAF tables,[35] and the enthalpy of formation of gaseous atomic Se, $\Delta_{f,0K}H^o(Se(g)) = 235.4 \pm 1.5$ kJ mol^{-1}.[13]

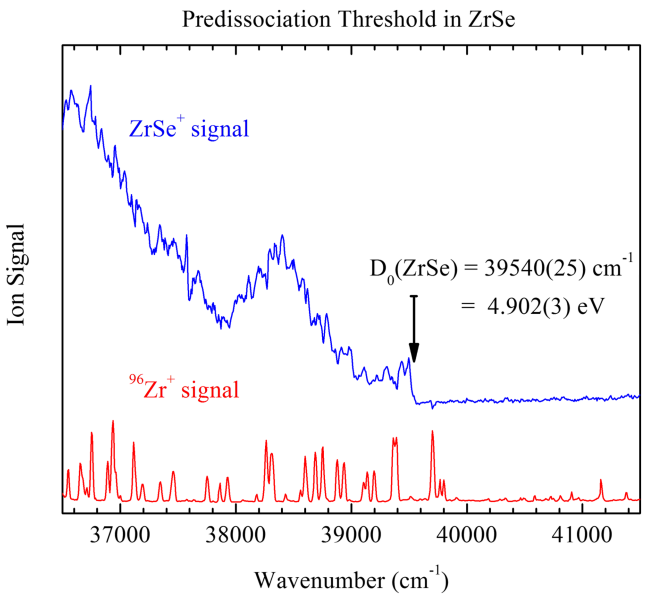

FIG. 3. Resonant two-photon ionization spectrum of $^{90}Zr^{80}Se$ (blue) along with the spectrum of the minor isotope ^{96}Zr (red), which was used for calibration.

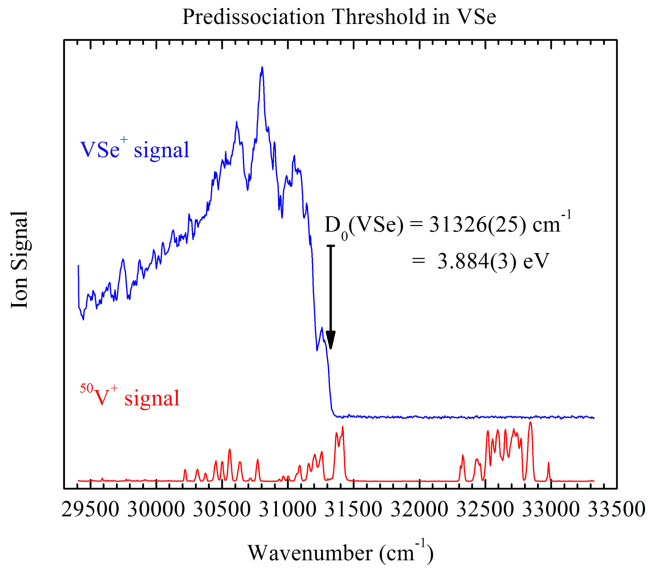

FIG. 5. Resonant two-photon ionization spectrum of $^{51}V^{80}Se$ (blue) along with the spectrum of the minor isotope ^{50}V (red), which was used for calibration.

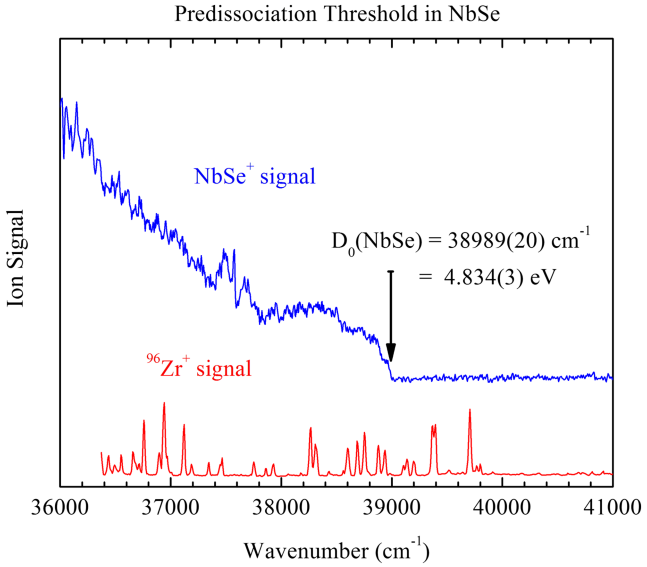

FIG. 6. Resonant two-photon ionization spectrum of $^{93}Nb^{80}Se$ (blue) along with the spectrum of the impurity ^{96}Zr (red), present in an earlier experiment, which was used for calibration.

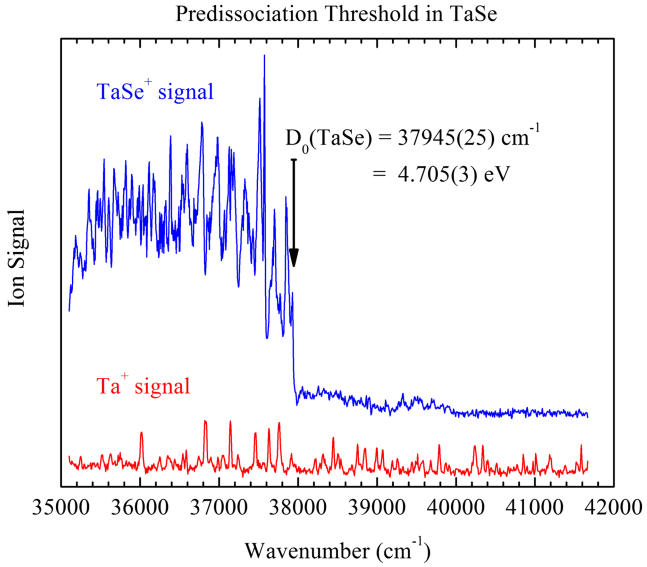

FIG. 7. Resonant two-photon ionization spectrum of $^{181}Ta^{80}Se$ (blue) along with the spectrum of ^{181}Ta (red), which was used for calibration. Because Ta has no minor isotopes of sufficient abundance to provide an atomic spectrum and the ^{181}Ta mass peak was quite intense, the calibration spectrum was obtained by recording the signal in the high-mass tail of this peak in the TOFMS.

We note that by far the largest contribution to the uncertainty in these values comes from the uncertainty in the enthalpy of formation of the gaseous metal atom. Table II also lists the spin-orbit corrected computed BDE using the B3LYP/LANL2DZ method, along with the deviation between this computed value and our measurement. It is obvious that this computational method fails badly in predicting the BDE for these molecules.

V. DISCUSSION

A. TiSe, ZrSe, and HfSe

Our calculations indicate that the ground terms for TiSe and ZrSe are $^3\Delta_1$ and the ground term for HfSe is $^1\Sigma^+_{0^+}$. In the cases of TiSe and HfSe, these ground state assignments conform to trends seen in the experimental ground states of TiO,[21] TiS,[24] HfO,[23] and HfS.[26] However, the expected ground state for ZrSe was $^1\Sigma^+_{0^+}$, based on the known ground states of ZrO and ZrS.[22,25]

As it turns out, a definitive assignment of the ground state symmetry is not necessary for the analysis of the predissociation threshold data in these particular molecules. The purpose of our calculations was to determine if any symmetry-based restrictions might exist that could make it difficult for the initially excited states to predissociate to atoms in their ground spin-orbit levels. For this analysis, we note that the ground separated atom limit for TiSe, ZrSe, and HfSe is d^2s^2, $^3F_{2g} + s^2p^4$, $^3P_{2g}$.[36] This separated atom limit produces molecular levels with $\Omega = 0^+, 0^-, 1, 2, 3$, and 4. If the ground molecular state is $^1\Sigma^+_{0^+}$, as is calculated for HfSe, then states with $\Omega = 0^+$ and 1 may be accessed in dipole-allowed transitions from the ground state. Both of these can dissociate to ground level atoms while preserving the Ω quantum number. Likewise, if the ground molecular state is $^3\Delta_1$, as is calculated for TiSe and ZrSe, molecular states with $\Omega = 0^+, 0^-, 1$, and 2 may be accessed in dipole-allowed transitions. Again, all of these can dissociate to ground level separated atoms while preserving the Ω quantum number. Even though there is some doubt concerning the ZrSe ground state, we can safely conclude that the excited states of ZrSe that are produced in our experiment can dissociate at the ground separated atom limit without requiring a change in Ω. Thus, we are confident that the

TABLE II. Measured BDEs, D_0, and enthalpies of formation, $\Delta_{f,0K}H^o$ for MSe molecules.

Molecule	D_0 (cm^{-1})	D_0 (kJ mol^{-1})	D_0 (eV)	$\Delta_{f,0K}H^o$(M(g)) (kJ mol^{-1})[a]	$\Delta_{f,0K}H^o$(MSe(g)) (kJ mol^{-1})[b]	Calculated D_0, with spin-orbit correction (eV)[c]	Computational error (eV)[d]
TiSe	32 242(50)	385.8(6)	3.998(6)	470.9 ± 17	320.6 ± 16.8	3.952	−0.046
ZrSe	39 540(25)	473.0(3)	4.902(3)	608.7 ± 8	371.1 ± 8.5	4.540	−0.362
HfSe	41 567(30)	497.3(4)	5.154(4)	618.0 ± 6	356.1 ± 6.5	4.306	−0.848
VSe	31 326(25)	374.8(3)	3.884(3)	512.2 ± 8	372.9 ± 8.1	3.553	−0.331
NbSe	38 989(20)	466.4(3)	4.834(3)	729.9 ± 8	498.9 ± 8.1	3.971	−0.863
TaSe	37 945(25)	454.0(3)	4.705(3)	781.5	562.9 ± 1.5	3.788	−0.917

[a]From Ref. 35.
[b]Computed using $\Delta_{f,0K}H^o$(Se(g)) = 235.4 ± 1.5 kJ mol^{-1}, from Ref. 13.
[c]See Section V D 2 for a description of how the spin-orbit correction to D_0 was estimated.
[d]Defined as the computed D_0, with spin-orbit correction, minus the measured D_0 value.

abrupt predissociation thresholds found in these molecules correspond to the true bond dissociation energies of the molecules.

The BDE for TiSe has previously been extrapolated from the BDEs of other titanium-containing molecules as D_0(TiSe) = 3.95(43) eV.[13] Wu, Wang, and Su also report a DFT calculated BDE for TiSe of D_0(TiSe) = 4.11 eV and we calculate a value of D_0(TiSe) = 4.082 eV (3.952 eV when estimated spin-orbit corrections are included).[14] Our experimental value, D_0(TiSe) = 3.998(6) eV, agrees well with the previous experimental estimate, but with a 70-fold reduction in the error limit. It also demonstrates that the BDEs calculated by Wu, Wang, and Su[14] and ourselves both lie within the range of expected chemical accuracy, if one adopts the looser standard suggested for transition metal molecules.[10] As far as we are aware, no previous work has been reported on the BDEs of either ZrSe or HfSe, for which we find D_0(ZrSe) = 4.902(3) eV and D_0(HfSe) = 5.154(4) eV. The calculated BDEs that we obtain using the B3LYP method and the LANL2DZ basis set, D_0(ZrSe) = 4.699 eV and D_0(HfSe) = 4.763 eV, are significantly lower than our experimental values. These computed values are in even greater disagreement with experiment when the effects of spin-orbit interaction are considered.

B. VSe and TaSe

The ground term of VSe was calculated to be $1\sigma^2\ 2\sigma^2\ 1\pi^4\ 1\delta^2\ 3\sigma^1$, $^4\Sigma^-$, giving $\Omega'' = 1/2$ and 3/2; the calculated ground term of TaSe was $1\sigma^2\ 2\sigma^2\ 1\pi^4\ 3\sigma^2\ 1\delta^1$, $^2\Delta$, giving $\Omega'' = 3/2$ for the lowest spin-orbit component. These ground levels lead to dipole-allowed transitions to states with $\Omega' = 1/2$, 3/2, or 5/2. Both VSe and TaSe have a ground separated atom limit of V/Ta, d^3s^2, $^4F_{3/2g}$ + Se, s^2p^4, $^3P_{2g}$,[36] which produces potential curves with $\Omega = 1/2$, 3/2, 5/2, and 7/2. Thus, any states that may be excited can predissociate to atoms in their ground spin-orbit levels while still preserving their Ω quantum number. Therefore, the sharp predissociation thresholds observed in VSe and TaSe may safely be assigned as the BDEs for these molecules.

The only previously reported BDE for VSe is D_0(VSe) = 3.55(22) eV, measured using Knudsen effusion mass spectroscopy.[12] Wu, Wang, and Su again report a value obtained from density functional calculations of D_0(VSe) = 3.76 eV, which agrees well with our calculated BDE of D_0(VSe) = 3.710 eV.[14] Our measured value, obtained from the observed predissociation threshold, is D_0(VSe) = 3.884(3) eV. This lies significantly outside the range of the previous measurement and shows that both the DFT result of Wu, Wang, and Su and our DFT result lie barely within the range required for chemical accuracy in calculations on transition metal molecules. When corrections for spin-orbit effects are included, the agreement between computation and experiment worsens. No previous experimental work has been done on the bond dissociation energy of TaSe, for which we find D_0(TaSe) = 4.705(3) eV. Again, our calculated BDE value of D_0(TaSe) = 4.101 eV is significantly smaller than the measured value, and the error becomes nearly 1 eV when spin-orbit corrections are included.

C. NbSe

As was found for VSe, the ground term of NbSe was calculated to be $1\sigma^2\ 2\sigma^2\ 1\pi^4\ 1\delta^2\ 3\sigma^1$, $^4\Sigma^-$, leading to possible Ω'' values of 1/2 and 3/2. Again, this gives dipole allowed transitions to excited states with $\Omega' = 1/2$, 3/2, or 5/2. The separated atom limit for NbSe differs from that of VSe and TaSe, however, and is Nb, d^4s^1, $^6D_{1/2g}$ + Se, s^2p^4, $^3P_{2g}$.[36] This limit leads to molecular states with Ω-values of $\Omega = 1/2$, 3/2, and 5/2. Just as was found for the previous molecules, all of the excited states that can be reached in excitations from the ground state can dissociate to the separated atoms in their ground levels while preserving the value of Ω. Again, we can be confident that the observed sharp predissociation threshold corresponds to the production of the separated atoms in their ground levels and is therefore a measurement of the actual bond dissociation energy of the molecule. On this basis, we assign D_0(NbSe) = 4.834(3) eV.

To our knowledge, no previous experimental work on the bond dissociation energy of NbSe has been reported. Our calculated BDE of D_0(NbSe) = 4.167 eV is much lower than the measured value, far outside the range required for chemical accuracy. When spin-orbit corrections are included, the error in the computed value again becomes significantly worse.

D. Error considerations

1. Experimental sources of error

The error limits quoted in this investigation are much smaller than those reported in other methods, so it is worthwhile describing the assumptions behind them. In general, errors can arise from either statistical uncertainties or errors of interpretation. The error limits presented for our values primarily reflect statistical uncertainties.

The atomic line positions that we use to calibrate our spectra are known to be 0.1 cm^{-1} or better;[36] this uncertainty is so small that it may be neglected. Our practice is to measure the line positions of a number of atomic lines that are close to the predissociation threshold, calculate the average error by comparing to the known wavenumbers, and then to shift the entire spectrum by the average error, to bring the atomic lines into alignment with their known positions. Of course, random deviations remain for the set of calibration lines. For the studies here, the rms errors in the shifted atomic line positions were less than 4 cm^{-1}. This is also negligible compared to other sources of error.

A second source of error arises because the ion signals shown in Figures 2–7 drop to baseline over a finite interval. We choose the predissociation threshold to lie near the midpoint of the final drop to baseline and assign an error limit that encompasses the range over which the final drop to baseline occurs. This procedure implicitly includes the uncertainty that arises from the laser linewidth, which is in the range of 15 cm^{-1} for atomic lines recorded under the conditions in which power broadening is minimized.

It might be thought that the existence of vibrationally excited molecules or rotationally warm molecules in the molecular beam could contribute to the uncertainty of the measurement, but we do not believe this to be the case. Vibrationally hot molecules would require a lower energy photon

to reach the dissociation threshold than cold molecules, so they would exhibit a predissociation threshold that is shifted to lower wavenumbers by the ground state vibrational quantum. Although a fraction of the molecules will undoubtedly be in $v'' = 1$, our past experience shows that this will be a small fraction, probably below 10%. As a result, vibrationally hot molecules would produce a weak preliminary threshold at lower wavenumbers, where it would be embedded in the ion signal due to cold molecules. This would be difficult to detect; if detected, it would be readily distinguished from the sharp final drop to baseline. Thus, we do not believe that a small fraction of vibrationally excited molecules can compromise our measurement.

It is a bit more complicated to consider rotationally excited molecules, but again we do not believe that rotational excitations will compromise our measurement significantly. Consider a ground state molecule with $J'' = 10$, for example. Such a molecule will possess a rotational energy of 110 B'', which could be roughly 10 cm^{-1} of energy. If the rotational energy could be fully utilized to reach the dissociation limit, this molecule would dissociate at a threshold roughly 10 cm^{-1} below that of a $J'' = 0$ molecule. However, when a $J'' = 10$ molecule is photoexcited, selection rules dictate that it will find itself in an excited state with $J' = 11$, 10, or 9. While nonadiabatic and spin-orbit coupling can allow this molecule to hop from one potential curve to another, the value of J' must be conserved. Furthermore, at long range, all potential curves associated with a given value of J' are dominated by the repulsive centrifugal potential given by

$$V(R) = \frac{J(J+1)\hbar^2}{2\mu R^2} = B(R)J'(J'+1). \quad (5.1)$$

The long-range nature of the centrifugal potential leads to a centrifugal barrier to dissociation. Thus, a molecule that is initially in a rotational level specified by J'' will experience a shift in the dissociation threshold compared to a cold molecule of roughly

$$\Delta E = B(R^*)J'(J'+1) - B''J''(J''+1). \quad (5.2)$$

Here R^* represents the internuclear separation that gives the highest point on the centrifugal barrier. Because the two terms are subtracted, we believe that any error associated with rotationally excited molecules in the beam will be small. Furthermore, because the top of the centrifugal barrier is expected to lie at a larger value of R^* than the ground state bond length, we expect $B(R^*) < B''$. As a result, the shift in the predissociation threshold for a rotationally hot molecule, given by (5.2), will be negative. The final drop to baseline therefore probably corresponds to the dissociation threshold for cold molecules because rotationally warm molecules will dissociate at slightly lower wavenumbers. The width of the drop to baseline probably results from the two primary effects: (1) the finite laser linewidth and (2) the population distribution of rotationally excited molecules in the beam, which experience a dissociation threshold shift given roughly by Equation (5.2). By choosing an error range that encompasses the width of the final drop of signal to baseline, we believe that our error limits are adequate to account for both effects.

The discussion of centrifugal barriers to dissociation brings up another point: how do we know that there are no other barriers to dissociation at the ground separated atom limit? This is a thorny issue, as we have no way of estimating the magnitude of any such barriers, and we assume they are nonexistent. It is certain that the predissociation thresholds observed in these studies represent an upper limit to the thermochemical BDE. If a barrier were present, however, the true thermochemical BDE could be lower than what we observe. As discussed in our study of the BDEs of VC, VN, and VS,[11] previous work on V_2 demonstrated through the use of a thermochemical cycle that any barrier in the predissociation of V_2 could be no larger than 0.002 eV. This is true despite the fact that V_2 is an example that might be expected to display a barrier. The ground separated atom limit of $3d^3 4s^2$, $^3F_2$ + $3d^3 4s^2$, $^3F_2$ is expected to be repulsive at long distances due to the Pauli repulsion of the filled $4s$ subshells. The fact that no substantial barrier exists in the case of V_2 gives us a reason to think that no substantial barrier to dissociation exists for the transition metal selenides as well. It would be useful to test this assumption by measuring precise BDEs for the transition metal selenide cations, MSe^+, along with the ionization energies of the MSe molecules, so that the thermochemical cycle

$$D_0(MSe) + IE(M) = IE(MSe) + D_0(M^+ - Se) \quad (5.3)$$

could be used to verify the lack of a barrier to dissociation, as has been done in the case of V_2.

2. Computational sources of error

It is also worthwhile to consider the possibility of errors in the computed BDEs of these molecules. A source of error that becomes more important for the heavier molecules is the neglect of spin-orbit interaction. Spin-orbit interaction stabilizes the $^3F_2$ levels of Ti, Zr, and Hf, the $^4F_{3/2}$ levels of V and Ta, the $^6D_{1/2}$ level of Nb, and the $^3P_2$ level of Se. Similarly, the $^3\Delta_1$ levels of TiSe, ZrSe, and HfSe and the $^2\Delta_{3/2}$ level of TaSe are also stabilized by spin-orbit interaction. The $^4\Sigma^-(\Omega = 1/2)$ levels of VSe and NbSe are likewise stabilized by spin-orbit interaction but only through their second-order interactions with other states. As a result, this will be less significant than in the other molecules, where first-order spin-orbit corrections to the energy are dominant. Similarly, spin-orbit stabilization of the $^1\Sigma^+$ states of TiSe, ZrSe, and HfSe cannot occur in first-order perturbation theory. Spin-orbit stabilization of the separated atoms has the effect of reducing the BDE from the computed value, while stabilization of the molecular ground state increases the BDE from the computed value.

The energy of the ground atomic term, E(L,S), in the absence of spin-orbit interaction, may be estimated as the degeneracy weighted average of the known energies of the spin-orbit levels,[36]

$$E(L,S) = \frac{\sum_J (2J+1)E(L,S,J)}{\sum_J (2J+1)}. \quad (5.4)$$

As the ground atomic level is at an energy defined to be zero, the spin-orbit stabilization of the ground level (taken to be a negative number, indicating stabilization) is −E(L,S) as

TABLE III. Corrections for spin-orbit stabilization of the ground atomic and molecular levels.[a]

Molecule	Electronic term	Term energy, T_e (eV)	ΔE^{SO}(atoms) (eV)	ΔE^{SO}(molecule) (eV)	ΔE^{SO}(atoms) – ΔE^{SO}(molecule)[b]
TiSe	$1\delta^1 3\sigma^1, {}^3\Delta\ (\Omega = 1)$	0	−0.145	−0.015	−0.130
	$3\sigma^2, {}^1\Sigma^+\ (\Omega = 0^+)$	1.27	−0.145	0.000	−0.145
ZrSe	$1\delta^1 3\sigma^1, {}^3\Delta\ (\Omega = 1)$	0	−0.207	−0.048	−0.159
	$3\sigma^2, {}^1\Sigma^+\ (\Omega = 0^+)$	0.43	−0.207	0.000	−0.207
HfSe	$3\sigma^2, {}^1\Sigma^+\ (\Omega = 0^+)$	0	−0.457	0.000	−0.457
	$1\delta^1 3\sigma^1, {}^3\Delta\ (\Omega = 1)$	0.53	−0.457	−0.196	−0.261
VSe	$1\delta^2 3\sigma^1, {}^4\Sigma^-\ (\Omega = 1/2, 3/2)$	0	−0.157	0.000	−0.157
	$1\delta^1 3\sigma^2, {}^2\Delta\ (\Omega = 3/2)$	1.27	−0.157	−0.022	−0.135
NbSe	$1\delta^2 3\sigma^1, {}^4\Sigma^-\ (\Omega = 1/2, 3/2)$	0	−0.196	0.000	−0.196
	$1\delta^1 3\sigma^2, {}^2\Delta\ (\Omega = 3/2)$	0.70	−0.196	−0.065	−0.131
TaSe	$1\delta^1 3\sigma^2, {}^2\Delta\ (\Omega = 3/2)$	0	−0.560	−0.247	−0.313
	$1\delta^2 3\sigma^1, {}^4\Sigma^-\ (\Omega = 1/2, 3/2)$	0.11	−0.560	0.000	−0.560

[a]The spin-orbit stabilization of the ground atomic levels, given by ΔE^{SO}(atoms), is described in the text. The spin-orbit stabilization of the ground molecular level, based on the electronic term, ignores second-order spin-orbit interactions and uses atomic spin-orbit parameters given by ζ_{3d}(Ti) = 123 cm^{-1}, ζ_{4d}(Zr) = 387 cm^{-1}, ζ_{5d}(Hf) = 1578 cm^{-1}, ζ_{3d}(V) = 177 cm^{-1}, ζ_{4d}(Nb) = 524 cm^{-1}, and ζ_{5d}(Ta) = 1995 cm^{-1}, taken from Ref. 37.

[b]The energy difference, ΔE^{SO}(atoms) – ΔE^{SO}(molecule), provides the correction that should be added to the calculated BDE that is obtained in a method that ignores spin-orbit interactions.

defined above. For convenience, the sum of the spin-orbit stabilization for the metal and selenium atoms is calculated from the known atomic energy levels and is listed in Table III as ΔE^{SO}(atoms).

To first order in perturbation theory, the spin-orbit stabilization of the ground molecular level is zero for the $^1\Sigma^+$ states of TiSe, ZrSe, and HfSe and for the $^4\Sigma^-$ states of VSe, NbSe, and TaSe. There is a first-order stabilization of the ground spin-orbit level in the $^3\Delta_1$ levels of TiSe, ZrSe, and HfSe and in the $^2\Delta_{3/2}$ levels of VSe, NbSe, and TaSe, however. Using the methods described by Lefebvre-Brion and Field,[37] it is readily shown that the spin orbit stabilization of the ground level in these $^3\Delta$ and $^2\Delta$ states may be estimated as $-\zeta_{nd}$, where ζ_{nd} is the spin-orbit constant for the n*d* atomic orbital of the metal atom. These values are tabulated in Ref. 37. The spin-orbit stabilization of the molecular state is also given in Table III as ΔE^{SO}(molecule).

The net spin-orbit correction to the BDE calculated using a computational method that ignores spin-orbit interaction is given by ΔE^{SO}(atoms) – ΔE^{SO}(molecule) and is listed in Table III for the various possible molecular ground states. In all cases the correction is negative, indicating that the inclusion of spin-orbit interaction will reduce the calculated BDE of the molecule. With the sole exception of TiSe, all of the BDEs calculated using the B3LYP/LANL2DZ method are already smaller than the measured values. The inclusion of spin-orbit corrections only worsens the agreement.

The fact that the spin-orbit correction depends critically on the electronic configurations of the separated atoms and of the bound molecule suggests that it will be difficult to develop a parameterization of density functional methods that can adequately treat a wide range of molecules, particularly those containing heavy atoms, unless spin-orbit interaction is explicitly included in the method.

E. General observations

In a previous study, we noted that in the multiply-bonded diatomic transition metals (Cr_2, V_2, CrW, NbCr, VNb, Mo_2, and Nb_2), a strong correlation exists between the *d*-orbital radial expectation value, $\langle r \rangle_{nd}$, and the bond dissociation energy, D_0.[38] It was rationalized that the main difficulty in achieving effective *d* orbital bonding arises from the small size of the *d* orbitals, particularly in relation to the valence *s* orbital. Larger *d* orbitals are able to overlap more effectively to make stronger bonds. For similar reasons, it is possible that the BDEs of the transition metal selenides might follow the same trend.

The small BDEs of TiSe and VSe are in keeping with this trend because the 3*d* metals have considerably smaller *d* orbital radii than their heavier 4*d* and 5*d* congeners. To consider this correlation more quantitatively, we note that the values of $\langle r \rangle_{nd}$ vary significantly with orbital occupation; the expectation value $\langle r \rangle_{nd}$ is larger in $d^{n+1}s^1$ configurations compared to $d^n s^2$ configurations, owing to the greater *d*-*d* electron repulsion in the former case. To account for this effect, we consider the 3σ molecular orbital to be purely of metal n*s* character and employ the $\langle r \rangle_{nd}$ value taken from the $d^{n+1}s^1$ configuration for molecules in which the 3σ orbital is singly occupied in the ground state. When the 3σ orbital is doubly occupied in the ground state, we employ the $\langle r \rangle_{nd}$ value taken from the computations of the $d^n s^2$ configuration instead. When possible, we have used the $\langle r \rangle_{nd}$ values obtained from numerical Dirac-Fock calculations, as tabulated by Desclaux.[39] These values differ slightly between the $d_{3/2}$ and $d_{5/2}$ orbitals; we have taken the average of the two values. When the appropriate electronic configuration was not included in this tabulation, we have scaled the numerical Hartree-Fock results of Charlotte Froese-Fischer by an interpolated value of the ratio of the relativistic $\langle r \rangle_{nd}$ value to the nonrelativistic one, as compiled by Desclaux.[39,40]

It seems likely that the ground terms of TiSe, VSe, and NbSe leave the 3σ orbital singly occupied, as is experimentally found in the analogues TiO, TiS, VO, VS, NbO, and NbS and as found in our calculations. Likewise, it is quite reasonable that the ground terms of HfSe and TaSe place two electrons in the 3σ orbital, as in the HfO, HfS, TaO, and TaS molecules and as found in our calculations. This is expected due to the relativistic stabilization of the 6s orbital in the metal atoms.

TABLE IV. Radial expectation values, $\langle r \rangle_{nd}$, for the $d^n s^2$ and $d^{n+1} s^1$ configurations.[a]

Transition metal	$d^n s^2$ (Å)	$d^{n+1} s^1$ (Å)	Transition metal	$d^n s^2$ (Å)	$d^{n+1} s^1$ (Å)
Ti	0.7931[b]	**0.9376**[c]	V	0.7200[b]	**0.8259**[c]
Zr	1.1563[b]	1.2733[c]	Nb	1.0410[c]	**1.1267**[b]
Hf	**1.2588**[b]	1.4112[c]	Ta	**1.1414**[b]	1.2365[c]

[a]Values in bold correspond to the likely ground configuration of the metal in the MSe molecule and are used in Figure 8.
[b]From Ref. 39.
[c]Estimated from Refs. 40 and 39.

In ZrSe, however, it is less certain whether the 3σ orbital is singly or doubly occupied. Our calculation suggests that it is singly occupied, while experimental data for the ZrO and ZrS analogues show it to be doubly occupied. Table IV provides the numerical Dirac-Fock calculated or estimated values of $\langle r \rangle_{nd}$ for the $d^n s^2$ and $d^{n+1} s^1$ configurations of the atoms. The bolded entries are used in Figure 8, where the measured bond dissociation energies are plotted vs. radial expectation value, $\langle r \rangle_{nd}$.

Figure 8 displays a striking correlation between bond dissociation energy and the *d*-orbital radial expectation value, similar to what was found for the multiply-bonded diatomic transition metals. The red line in the figure represents a fitted line through the data points for TiSe, HfSe, VSe, NbSe, and TaSe, where the molecular configuration seems definite. For ZrSe, we have plotted the data points obtained for $\langle r \rangle_{nd}$ calculated for both the $4d^2 5s^2$ (blue open square) and $4d^3 5s^1$ (red open circle) configurations of atomic Zr. If the trend holds for ZrSe, this plot suggests that the ground state of this molecule places two electrons in the 5*s*-like 3σ orbital, giving a $1\sigma^2\ 2\sigma^2\ 1\pi^4\ 3\sigma^2$, $^1\Sigma^+$ ground term, as is experimentally found in ZrO and ZrS.

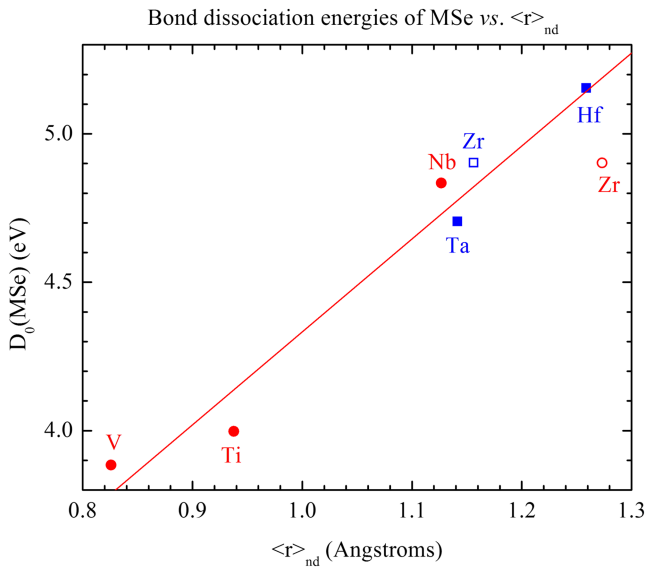

FIG. 8. Correlation of bond dissociation energy with radial expectation value, $\langle r \rangle_{nd}$. Values obtained from $d^n s^2$ configurations are shown as blue squares and those obtained from $d^{n+1} s^1$ configurations are shown as red circles. Because of the ambiguity of whether the 3σ orbital is singly occupied or doubly occupied in the ground state of ZrSe, points are plotted using the values of $\langle r \rangle_{nd}$ for both the $4d^2 5s^2$ (blue open square) and $4d^3 5s^1$ (red open circle) configurations of this atom.

The correlation of bond dissociation energy and *d*-orbital radial expectation value seems too simplistic to completely account for the chemical bonding in these molecules. For example, it ignores differences in the ionization energy of the metal atom, which is clearly relevant to the ionic contributions to the chemical bonding. While five of the metals examined here have ionization energies in the range 6.73 ± 0.10 eV, tantalum has a significantly higher ionization energy, 7.55 eV. The higher ionization energy of tantalum apparently does not significantly influence its ability to bond to selenium, however. Likewise, this correlation neglects any differences in the promotion energy required to prepare the atoms for bonding and ignores any differential stabilization of the separated atom limit *vs*. the MSe molecule due to spin-orbit effects. All of these effects are undoubtedly important, but fail to show up in the simple correlation found in Figure 8. We hope to test this correlation further by studies on the group 3 transition metal selenides, ScSe, YSe, and LaSe.

VI. CONCLUSION

Predissociation thresholds for TiSe, ZrSe, HfSe, VSe, NbSe, and TaSe were observed using resonant two-photon ionization spectroscopy, and from these observations, bond dissociation energies and enthalpies of formation were derived. Along with the previous work on the BDEs of VC, VN, and VS and forthcoming work on the BDEs of TiSi, ZrSi, HfSi, VSi, NbSi, and TaSi, these studies have shown that the onset of predissociation in a congested vibronic spectrum provides a reliable means of estimating the bond dissociation energy for many MC, MN, MSi, MS, and MSe molecules. We believe that this method is likely to succeed for any transition metal atom (including lanthanides and actinides) where the ground term of the transition metal atom is a highly degenerate D, F, or higher term. While transition metals with ground S terms will likely be problematic (Cr, Mo, Mn, Tc, Re, Pd, Cu, Ag, Au, Zn, Cd, and Hg), the method is highly promising for molecules containing the remaining transition metals (Sc, Y, La, Ti, Zr, Hf, V, Nb, Ta, W, Fe, Ru, Os, Co, Rh, Ir, Ni, Pt, and most of the lanthanides and actinides).

ACKNOWLEDGMENTS

The authors thank the National Science Foundation for support of this research under Grant No. CHE-1362152. We also thank Professors Richard Ernst and Thomas Richmond for their assistance in the synthesis of gaseous H_2Se.

[1]X. Cong, C. Cheng, Y. Liao, Y. Ye, C. Dong, H. Sun, X. Ji, W. Zhang, P. Fang, L. Miao, and J. Jiang, J. Phys. Chem. C **119**, 20864–20870 (2015).
[2]R. Lv, J. A. Robinson, R. E. Schaak, D. Sun, Y. Sun, T. E. Mallouk, and M. Terrones, Acc. Chem. Res. **48**, 56–64 (2015).
[3]H. M. Choi, I. A. Ji, and J. H. Bang, ACS Appl. Mater. Interfaces **6**, 2335–2343 (2014).
[4]J. Guo, S. Liang, Y. Shi, C. Hao, X. Wang, and T. Ma, Phys. Chem. Chem. Phys. **17**, 28985–28992 (2015).
[5]K. N. Uttam, R. Gopal, and M. M. Joshi, Pramana **43**, 73–80 (1994).
[6]L. C. O'Brien, A. K. Lambeth, and C. R. Brazier, J. Mol. Spectrosc. **213**, 64–68 (2002).
[7]S. Manivasagam, M. L. Laury, and A. K. Wilson, J. Phys. Chem. A **119**, 6867–6874 (2015).
[8]X. Xu, W. Zhang, M. Tang, and D. G. Truhlar, J. Chem. Theory Comput. **11**, 2036–2052 (2015).

[9]M. L. Laury and A. K. Wilson, J. Chem. Theory Comput. **9**, 3939–3946 (2013).
[10]N. J. DeYonker, K. A. Peterson, G. Steyl, A. K. Wilson, and T. R. Cundari, J. Phys. Chem. A **111**, 11269–11277 (2007).
[11]E. L. Johnson, Q. C. Davis, and M. D. Morse, J. Chem. Phys. **144**, 234306-1–234306-9 (2016).
[12]C. Bergman, P. Coppens, J. Drowart, and S. Smoes, Trans. Faraday Soc. **66**, 800–808 (1970).
[13]A. Olin, B. Nolang, G. Osadchii *et al.*, *Chemical Thermodynamics of Selenium* (Elsevier, OECD Nuclear Energy Agency, 2005).
[14]Z. J. Wu, M. Y. Wang, and Z. M. Su, J. Comput. Chem. **28**, 703–714 (2007).
[15]W. C. Wiley and I. H. McLaren, Rev. Sci. Instrum. **26**, 1150–1157 (1955).
[16]B. A. Mamyrin, V. I. Karataev, D. V. Shmikk, and V. A. Zagulin, Zh. Eksp. Teor. Fiz. **64**, 82–89 (1973).
[17]M. J. Frisch, G. W. Trucks, H. B. Schlegel, G. E. Scuseria, M. A. Robb, J. R. Cheeseman, G. Scalmani, V. Barone, B. Mennucci, G. A. Petersson, H. Nakatsuji, M. Caricato, X. Li, H. P. Hratchian, A. F. Izmaylov, J. Bloino, G. Zheng, J. L. Sonnenberg, M. Hada, M. Ehara, K. Toyota, R. Fukuda, J. Hasegawa, M. Ishida, T. Nakajima, Y. Honda, O. Kitao, H. Nakai, T. Vreven, J. A. Montgomery, Jr., J. E. Peralta, F. Ogliaro, M. Bearpark, J. J. Heyd, E. Brothers, K. N. Kudin, V. N. Staroverov, R. Kobayashi, J. Normand, K. Raghavachari, A. Rendell, J. C. Burant, S. S. Iyengar, J. Tomasi, M. Cossi, N. Rega, N. J. Millam, M. Klene, J. E. Knox, J. B. Cross, V. Bakken, C. Adamo, J. Jaramillo, R. Gomperts, R. E. Stratmann, O. Yazyev, A. J. Austin, R. Cammi, C. Pomelli, J. W. Ochterski, R. L. Martin, K. Morokuma, V. G. Zakrzewski, G. A. Voth, P. Salvador, J. J. Dannenberg, S. Dapprich, A. D. Daniels, Ö. Farkas, J. B. Foresman, J. V. Ortiz, J. Cioslowski, and D. J. Fox, GAUSSIAN 09, Revision D.01, Gaussian, Inc., Wallingford, CT, 2009.
[18]C. Lee, W. Yang, and R. G. Parr, Phys. Rev. B: Condens. Matter Mater. Phys. **37**, 785–789 (1988).
[19]A. D. Becke, J. Chem. Phys. **98**, 5648–5652 (1993).
[20]P. J. Hay and W. R. Wadt, J. Chem. Phys. **82**, 299–310 (1985).
[21]W. H. Hocking, M. C. L. Gerry, and A. J. Merer, Can. J. Phys. **57**, 54–68 (1979).
[22]P. D. Hammer and S. P. Davis, Astrophys. J. **237**, L51–L53 (1980).
[23]L. A. Kaledin, J. E. McCord, and M. C. Heaven, J. Mol. Spectrosc. **173**, 37–43 (1995).
[24]J. Jonsson and O. Launila, Mol. Phys. **79**, 95–103 (1993).
[25]B. Simard, S. A. Mitchell, and P. A. Hackett, J. Chem. Phys. **89**, 1899–1904 (1988).
[26]O. Launila, J. Jonsson, G. Edvinsson, and A. G. Taklif, J. Mol. Spectrosc. **177**, 221–231 (1996).
[27]A. S. C. Cheung, A. W. Taylor, and A. J. Merer, J. Mol. Spectrosc. **92**, 391–409 (1982).
[28]J. L. Femenias, G. Cheval, A. J. Merer, and U. Sassenberg, J. Mol. Spectrosc. **124**, 348–368 (1987).
[29]C. J. Cheetham and R. F. Barrow, Trans. Faraday Soc. **63**, 1835–1845 (1967).
[30]Q. Ran, W. S. Tam, A. S. C. Cheung, and A. J. Merer, J. Mol. Spectrosc. **220**, 87–106 (2003).
[31]O. Launila, J. Mol. Spectrosc. **229**, 31–38 (2005).
[32]S. Wallin, G. Edvinsson, and A. G. Taklif, J. Mol. Spectrosc. **192**, 368–377 (1998).
[33]L. A. Kaledin, J. E. McCord, and M. C. Heaven, J. Mol. Spectrosc. **174**, 93–99 (1995).
[34]L. A. Kaledin, J. E. McCord, and M. C. Heaven, J. Mol. Spectrosc. **173**, 499–509 (1995).
[35]M. W. Chase, Jr., *NIST-JANAF Thermochemical Tables*, 4th ed. (American Institute of Physics for the National Institute of Standards and Technology, Washington, DC, 1998).
[36]A. E. Kramida, Y. Ralchenko, J. Reader, and NIST ASD Team, NIST Atomic Spectra Database, version 5.3, National Institute of Standards and Technology, Gaithersburg, MD, 2015.
[37]H. Lefebvre-Brion and R. W. Field, *The Spectra and Dynamics of Diatomic Molecules* (Elsevier, Amsterdam, 2004).
[38]D. J. Matthew, S. H. Oh, A. Sevy, and M. D. Morse, J. Chem. Phys. **144**, 214306-1–214306-10 (2016).
[39]J. P. Desclaux, At. Data Nucl. Data Tables **12**, 311 (1973).
[40]C. F. Fischer, *The Hartree-Fock Method for Atoms* (John Wiley & Sons, New York, 1977).